[May 04, 2010]

A PCR REACTOR WITH AN INTEGRATED ALUMINA ISOLATION MEMBRANE

Jitae Kim[a], Michael Mauk[a], Dafeng Chen[a], Xianbo Qiu[a], Jungkyu Kim[b], Bruce Gale[b], and Haim H. Bau[a,c]

a. Department of Mechanical Engineering and Applied Mechanics, University of Pennsylvania, Philadelphia, PA 19104-6315
b. Department of Mechanical Engineering, University of Utah, Salt Lake City, UT 84112
c. Corresponding author (bau@seas.upenn.edu)

ABSTRACT

Recently, there has been a growing interest in point of care devices capable of detecting nucleic acids in clinical and environmental samples. Nucleic acid detection requires, however, various sample preparation steps that complicate device operation. An attractive remedy is to integrate many, if not all, sample preparation operations and nucleic acid amplification into a single reaction chamber. A microfluidic chip that integrates, in a single chamber, polymerase chain reaction (PCR) amplification with solid-phase extraction of nucleic acids using a nanoporous, aluminum oxide membrane (AOM) is described. Samples suspected of containing target bacteria and/or viruses are mixed with lysis agents and a chaotropic salt and loaded into a plastic chip housing a nanoporous, aluminum oxide membrane. The nucleic acids in the lysate bind to the membrane. The membrane is then washed, the chamber is filled with the PCR reaction reagents, and the chamber's temperature is cycled to amplify the captured nucleic acids and produce detectable products. Both DNA and RNA (with reverse-transcription) isolation and amplification are demonstrated. Due to the dry membrane's high resistance to liquid flow, a specialized flow control system was devised to facilitate sample introduction and membrane washing.

Keywords: Lab on a chip, Point of care, diagnostic device, PCR, RT, HIV, virus, bacteria

1. Introduction

Assays based on sequence specific detection of nucleic acids (DNA and RNA) are increasingly becoming an important component of medical diagnostics, environmental monitoring, and food quality testing. Nucleic acid-based assays provide higher sensitivity and specificity than immunoassays. Nucleic acid-based tests may also exclude the presence of disease even when antibodies are present in the sample due to prior exposure to the pathogen. In certain cases such as HIV infection [Fiebig et al., 2003], antibodies may be present in detectable quantities only several weeks after infection leaving the disease undetected while the patient carries a high viral load and is highly infectious. Nucleic acid sequences specific to viral and bacterial pathogens, bioterrorism agents, genetic diseases, and aberrant gene expression can be assayed with high sensitivity because the enzymatic amplification increases the concentration of target analytes, thereby facilitating detection by fluorescence, optical absorption, chemoluminescence, and other chemical, electrochemical, or physical means.

Nucleic acid based diagnostics rely on sample preparation to yield target nucleic acids in a sufficiently pure and concentrated form for enzymatic amplification and/or reverse transcription. Briefly, prior to amplification or reverse transcription, the sample is lysed to release the target nucleic acid from virus particles or cells contained in the sample. The solubilized nucleic acids are then extracted from the heterogeneous lysate and washed to remove contaminants and other interfering compounds that are either intrinsic to the sample or have been added to the sample to facilitate lysis and binding and to stabilize the analytes (e.g., deactivate nucleases).

Pathogen and other disease-related nucleic acids typically encountered in clinical specimens such as blood, saliva, and urine and in environmental samples such as water dictate sample volumes on the order of hundreds of microliters to assure the presence of a sufficient quantity of target analytes in the sample. On the other hand, the PCR reaction chamber's volume is usually limited to ~10 microliters due to the reagents' high cost and the difficulty of facilitating rapid thermal cycling and temperature uniformity (± 0.5 °C) in larger reaction chambers. Consequently, an important function of the sample preparation process is to concentrate the target molecules to bridge the mismatch between the sample volume (10 to 1000 μl) and the PCR reaction chamber's volume (1-25 μl). The isolation step must provide ten-fold or more reduction in lysate volume, without significant loss of nucleic acids.

Currently, the method of choice for nucleic acid isolation relies on solid-phase extraction with porous silica as the nucleic acid binding phase. The sample is mixed with reagents, such as chaotropic salts (i.e., guanidinium chloride), that promote binding of the nucleic acids to the solid phase such as glass fibers, silica beads, and silica gel. The bound nucleic acid is then washed to remove lysate debris and lysing agents, and then eluted in a form suitable for amplification by PCR.

Silica-based spin column kits are the most common benchtop method of nucleic acid isolation for PCR and RT-PCR [Bowen and Durre, 2003]. A typical spin column comprises a ~5 mm diameter, ~1 mm thick glass fiber disc (membrane), or other form of silica, mounted in a polypropylene tube. Spin columns use either low-speed centrifugation or vacuum suction to facilitate flow through the porous silica membrane. The sample is first lysed with a chaotropic salt, enzymes, and detergents, and loaded into the spin column, where it flows through the porous silica membrane that binds nucleic acids contained in the lysate. The loading step is followed by flow-through of wash and elution buffers. A fraction of the eluted liquid, containing nucleic acids in a relatively pure form, is mixed with PCR reagents and thermal-cycled for amplification in a separate chamber.

The silica membrane's size and the loading, wash, and elution buffers' volumes must be optimized to achieve acceptable nucleic acid yield (>50%). The membrane must be sufficiently large to bind a high fraction of the nucleic acids from the lysate, but not too large to hinder desorption and release of nucleic acids from the membrane when using a relatively small elute volume. With just a very few exceptions (e.g., Hourfar *et al.*, 2005), wash buffers contain ethanol. Since ethanol is a strong inhibitor of PCR, it is critical to remove the residual ethanol from the membrane prior to nucleic acid elution so as to avoid contamination of the PCR reaction with ethanol. Ethanol in the reaction mix adversely affects amplification efficiency.

Although there are numerous reports on adapting silica-based, solid-phase extraction processes to microfluidic devices [Christel *et al.*, 1999; Wolfe *et al.* 2002; Breadmore *et al.*, 2003; Cady *et al.*, 2003; Chen *et al*., 2004; and Wang *et al.*, 2005], there are just a few reports on integrating the PCR chamber with upstream silica-based extraction and elution of nucleic acids [Easley *et al.*, 2006; Chen *et al.*, 2007; Liu *et al.*, 2009, Chen et al., 2010, and references cited therein].

It has been our experience (Chen et al., 2010) that complete removal of residual ethanol from a silica membrane integrated in a microfluidic system is difficult, and the presence of residual ethanol in the elution is more acute than in benchtop operation. In the benchtop 200 µl sealed PCR capsule, there is an air-pocket above the 20-50 µl liquid reaction mix, which accommodates the volatilization of ethanol. In contrast, the microfluidic PCR chamber is typically completely filled with liquid and sealed. Thus, it does not allow any residual ethanol to escape adversely impacting amplification efficiency. Typical microfluidic ethanol removal strategies include washing with high salt solution, drying with heated air, and discarding the first (target-rich) fraction of the elution [Legendre, *et al.*, 2006]. Too stringent a wash and the discarding of the first, nucleic acid-rich fraction of the elution cause loss of valuable target. Given the complexity of the silica-based extraction process in microfluidics, it is desirable to consider alternatives.

Burgoyne [2001] described the use of nitrocellulose filter paper to isolate nucleic acids. In this method, a raw (untreated) sample is blotted on nitrocellulose paper containing dried detergents and salts which function as lysing agents. The filter paper is washed with ethanol-containing buffers to remove proteins, lysate debris, and lysing agents, and then a 1- to 2-mm disc containing bound nucleic acid target is punched from the filter paper and added directly to a 50-µl PCR reaction mix. No separate elution step is needed. As long as the nitrocellulose membrane disc's volume is sufficiently small compared to the volume of the PCR reactor, the disc does not severely inhibit the PCR amplification. In contrast, silica membrane in direct contact with the PCR reaction strongly inhibits amplification, thus precluding the direct *in-situ* PCR amplification of nucleic acids bound to a silica membrane. Thus, silica membrane-based isolation must be carried out in a separate chamber upstream of the PCR chamber, which complicates flow control and adds cost.

Another promising approach for nucleic acid extraction is to use a nucleic isolation membrane made of porous aluminum oxide [Gerdes *et al*, 2001]. At high salt concentration, the alumina binds nucleic acids tightly. Once the alumina phase is immersed in a PCR reaction mix, the immobilized nucleic acids provide a template for PCR. The nucleic acids bound to an alumina solid phase can be repeatedly used as a template for successive PCRs. Therefore, Gerdes surmises that the nucleic acids remain bound to the membrane during the thermal cycling process. Margraf *et al.* [2004] adapted Gerdes *et al*.'s technology for a benchtop, single-tube nucleic acid

extraction, amplification, and sequencing of hepatitis C virus. Elgort *et al.* [2004] used Whatman Nanopore®, 8 mm^2 discs of an aluminum oxide membrane (AOM) mounted in wells as filtration "cards". A lysate, formed by mixing 1 μl of whole blood with 200 mM NaCl, 10 mM Triton X, and proteinase K, for a total volume of 100 μl, was filtered through the AOM, and washed with 200 mM NaCl. The membrane was then added to a PCR reaction tube for amplification. Dames *et al.* [2006] modified a 200-μl PCR tube to include a mounted AOM disc for benchtop, single-tube nucleic acid extraction, real-time PCR amplification, and detection. The chaotropic lysis/binding buffer consisted of either 5.5 M guanidine HCl, 50 mM Tris-HCl, 20 mM EDTA, 1.3% Triton X-100 or Qiagen AL buffer. The AOM was washed with 200 μl of 200 mM NaCl and 200 μl of water. Kim *et al.* [2006, 2008] developed a DNA extraction chip with an AOM membrane and studied the membrane's retention capacity. Working with raw blood samples, they demonstrated extraction efficiency of nearly 90%. The eluted DNA was amplified in a benchtop PCR reactor demonstrating that the process did not degrade the DNA. The integration of DNA extraction and amplification has not been explored. Erali *et al.* [2004] noted that although the autofluorescence of AOM is higher than that of glass and silica, it is lower than that of other polymers and could be further suppressed with appropriate chemical treatments, thus permitting *in-situ* detection using fluorimetry and real-time PCR. The absence of ethanol in the wash buffers and the elimination of a separate elution step are major advantages of the AOM for microfluidics implementations.

In summary, the above cited works indicate that nanoporous aluminum oxide membranes (**AOM**) are attractive for microfluidic implementations of molecular diagnostics since they have a good nucleic acid binding capacity, can be used in a continuous filtration mode to isolate nucleic acids from large sample volumes, are compatible with conventional PCR and real-time PCR, and do not require wash buffers that contain ethanol or other PCR inhibitors. On the other hand, the implementation of alumina membranes in a microfluidic chip presents technical challenges since the material is brittle and requires careful handling and the small pores, typically ranging in diameter from 20 nm to 200 nm, present high resistance to through flow when dry.

In this paper, we report on a microfluidic module containing a PCR reactor with integrated solid-phase extraction of nucleic acids based on a porous aluminum oxide membrane. The sample, mixed with lysis and binding agents, flows through the membrane in a continuous

filtration mode. The nucleic acids are extracted from a relatively large volume of sample. After washing, the membrane with the bound nucleic acid is exposed to the PCR reaction mix and subjected to thermal cycling to amplify the membrane-bound nucleic acids. A flow control algorithm has been developed to overcome the high resistance of the dry membranes to fluid flow. The operation of the device was demonstrated by isolating and amplifying bacterial genomic DNA and isolating, reverse transcripting, and amplifying viral RNA.

2. Materials and Methods

2.1 PCR Module with Integrated Nucleic Acid Isolation

The AOM chip was fabricated with four layers of CNC-machined, polycarbonate (PC) plastic sheets. **Fig. 1A** depicts an exploded view of the PCR module. Layer 1 (250 μm thick) formed the bottom surface of the reactor. The reactor chamber and the connecting conduits were milled in the 800 μm thick layer 2. The conduits were milled on both sides of layer 2. Layer 3 (250 μm thick) contains vertical vias. Layer 4 (500 μm thick), which also contains vertical vias, is used to increase the rigidity of the structure. Layers 1 and 3 were made of thin PC sheets to reduce thermal resistance.

AOM discs, 5.0 mm in diameter, were cut with a CO_2 laser (Univeral Laser Systems, Scottsdale, Arizona) from a 65 μm thick aluminum oxide membrane (100 nm diameter pores, Whatman Anodisc 25). The disks were inserted into the PCR chamber. **Fig. 1B** depicts the cross-section of the PCR module. A ledge milled in layer 2 supported the alumina membrane disc. Prior to the membrane's placement in the PCR chamber, a thin layer of molten paraffin (Ampliwax® PCR Gems, Roche, Nutley, NJ, melting point ≅ 65 °C) was coated along the surface of the ledge. Then, the alumina disk was placed on top of the paraffin. The entire device was heated to above 80 °C to melt the paraffin. Upon cooling, the AOM membrane was sealed in position. This particular sealing technique was used to prevent the shattering of the fragile membrane during assembly. The paraffin seal prevented any fluid flow around the membrane disc when the module operated in filtration mode. The paraffin's melting during the thermal cycling process was of no concern since the paraffin is PCR compatible and during the PCR phase, the sealing of the membrane is not needed. As an alternative, it is anticipated that in mass

production, the alumina membrane will be formed by thin-film deposition of the aluminum layer directly on the plastic.

The various layers were bonded with solvent (acetonitrile) at room temperature. **Fig. 1C** shows a photograph of the assembled PCR module containing the AOM for the isolation of nucleic acids. The resulting PCR chamber, partitioned by the AOM into lower and upper compartments, had a height of 800μm, and a volume ranging from 15 to 30 μl. The membrane's position, measured from the bottom of the PCR chamber, was at about a third of the chamber's height. The various ports, denoted V_1, V_2, V_3, and V_4, were connected to independently controlled valves. Hydraulic valves specifically designed for this purpose are described elsewhere [Kim *et al.*, 2009]. Each reactor was used just once and disposed after use.

2.2 PCR Module's Flow and Thermal Control

The PCR module's operation comprised the following steps: (*i*) loading into the PCR chamber a mixture consisting of lysate and binding agents (to promote the binding of the nucleic acid to the alumina membrane); (*ii*) washing the membrane; (*iii*) loading the PCR/RT-PCR mix; and (*iv*) thermal cycling.

Initially, ports V_1 and V_3 were open and ports V_2 and V_4 were closed (**Fig. 2A**). Lysate, mixed with binding buffer, entered the chamber through port V_1 and filled the upper part of the PCR compartment. Once the membrane was completely wet, the lysate (~ 23.5 μl) filtered through the membrane at a flow rate of about 4.7 μl/min and left the PCR compartment through port V_3. During this process, nucleic acids in the lysate bound to the alumina membrane's surface. Then, all the ports were opened. Wash solution (200 mM KCl) was introduced concurrently through ports V_1 and V_4 and exited through ports V_2 and V_3 (**Fig. 2B**). Next, the residual wash solution was expelled from the chamber with forced air. Although one could use the PCR mix to displace the wash solution, we used air to prevent the PCR reagents from being contaminated with wash solution. To mitigate concerns of air-borne contamination, the relatively small amount of air needed for the drying process could be supplied from a purified source or filtered through a membrane. In our experiments, negative controls (samples without targets) did not yield any amplicons. Therefore, we assume that air-borne contamination did not significantly affect the results of our experiments. Subsequently, PCR mix was supplied

concurrently through ports V_1 and V_4 (**Fig. 2C**). Finally, all the ports were sealed and reactor's temperature was cycled (**Fig. 2D**).

The thermal cycling was carried out by sandwiching the AOM-PCR module between two thermoelectric units (Melcor, Trenton, NJ). Heating from both below and above was used to minimize temperature nonuniformities along the reactor's height and to increase the ramping rate above what would have been possible with a single heater. The thermoelectric units were controlled with a custom-written LabVIEW™ (National Instruments, Austin, TX) program. For additional details, see Kim *et al.* [2009].

2.3 Membrane's Retention Capacity

The membrane's retention capacity for DNA molecules was reported elsewhere [Kim et al., 2006 and 2008]. To test the membrane's RNA binding capacity, we measured the fraction of RNA molecules retained by the membrane. The experiments were carried out with the AOM-PCR modules described in section 2.1. Armored RNA was extracted using High Pure™ Viral RNA protocol (Roche, USA). The binding buffer (Roche kit, 4.5 M guanidine-HCl, 50 mM Tris-HCl, 30% Triton® X-100 (w/v), pH 6.6) was mixed with Poly A oligotides (provided in the Roche kit) at a 100:1 volume ratio. Then, 400 copies/μl of purified armored RNA was added to the binding buffer-Poly A mixture at a 2:1 volume ratio, and the mixture was immediately treated with ZAP spray (Sigma Aldrich, USA) to remove any RNase. After incubating the mixture for 10 min, 100 μl of the mixture was pumped through the membrane embedded in the microfluidic system with a syringe pump (KD Scientific Inc., MA, USA). The discharged liquid that passed through the system was collected and immediately stored at -4 °C. To quantify the RNA in the initial sample and the unbound RNA, we carried out a Ribogreen™ fluorescence assay (Invitrogen, USA). Consistent with the Invitrogen protocol, all samples were inserted in wells of a 96-well plate and the fluorescence intensity was read with a Synergy™ HT, multi-mode microplate reader (BioTek Instruments Inc., USA).

2.4 Bacterial Target

The DNA target consisted of *B. Cereus* (American Type Culture Collection, Manassas, VA, USA, ATCC #27522) cell culture ($\cong 10^8$ cells per ml as determined by hemocytometery)

diluted to various concentrations by mixing with appropriate volumes of buffer. The DNA sample was prepared by incubating 11 μl of the *B. Cereus* cell culture with 1.5 μl Proteinase K and 11 μl Qiagen AL buffer (~6 M Guanidinium HCl) for 25 minutes at 56 °C. After the binding step, the AOM-PCR module was washed with 70 μl, 200 mM KCl solution for one minute at room temperature followed by blowing air for about four minutes.

The PCR mix consisted of 1½ illustra™ pure Taq Ready-To-Go PCR beads, (GE Healthcare), 0.75 μl of 0.10 mM forward primer 5'-TCT CGC TTC ACT ATT CCC AAG T-3', 0.75 μl of 0.10 mM reverse primer (5'-AAG GTT CAA AAG ATG GTA TTC AGG-3' (Operon Biotechnologies, Huntsville, AL), and 0.5 μl PEG-8000 (polyethylene glycol, 8000 molecular weight; Sigma Aldrich, USA) as a surface passivant [Lou et al., 2004]. When dissolved in a 25 μl reaction volume, each PCR bead provides 2.5 units of Taq polymerase; 200 μm of each dNTP; 10 mM Tris-HCl, pH 9.0; 50 mM KCL and 1.5 mM $MgCl_2$). The PCR thermal cycling comprises 20 s denaturation at 94 °C , 28 s annealing at 55 °C, and 37 s extension at 72 °C (including ramping times) with 35 cycles. Neither the buffers nor the cycling time were optimized.

2.5 RNA Target

The RNA sample was prepared by incubating 2 μl RNA isolated from Asuragen (Austin, TX) Armored RNA® HIV surrogate (RNAse-resistant ≅360-base ss-RNA of HIV gene sequence with primer binding sites packaged in a protein coat) at various concentrations with 6 μl DI water and 16 μl Qiagen AL buffer (~6 M Guanidinium HCl) for 10 minutes at 56 °C. After the binding process, the AOM-PCR module was washed with 100 μl, 200 mM KCl solution for one minute at room temperature followed by air drying for about four minutes.

The PCR mix consisted of reagents provided with the Promega (Madison, WI) Access® RT-PCR kit comprising AMV/ Tfl reaction buffer, 0.2 mM dNTP mix, 0.1 unit/μl AMV reverse transcriptase, 0.1 unit/μl DNA polymerase, 25 mM MgSO4, along with 0.75 μL of 0.1 mM primers: 5'-TACTAGTAGTTCCTGCTATGTCACTTCC-3' and 5'-AGTGGGGGGACATCAAGGCAGCCATGCAAAT-3' (Operon Biotechnologies, Huntsville AL), and 0.5 μL PEG (Sigma Aldrich, USA). The PCR thermal cycle consisted of 20 min reverse transcription at 50 °C, 20 s denaturation at 95 °C, 40 s annealing at 58 °C, and 50 s

extension at 72 °C (including ramping times) with 35 cycles. Neither the buffers nor the cycling time were optimized.

3. Results and Discussion

3.1 AOM Inhibitory Effect

The novel feature of this work is the direct amplification of the membrane-captured nucleic acid targets by contacting the PCR reaction mix with the loaded membrane. Generally, nucleic acid-binding phases, such as silica, nitrocellulose, aluminum oxide, and most polymers, are expected to exhibit some degree of PCR inhibition since they are likely to immobilize enzymes and primers in addition to the nucleic acid template. These effects are partially mitigated by the high temperatures (50-95 °C), elevated pH (7-8), and low salt concentration (~100 mM) of the PCR reaction, which promote desorption of nucleic acids from the membrane's surface. To determine a reasonable size for the AOM disk, we carried out benchtop, real-time PCR experiments in tubes containing 50 μl of PCR reaction volume and 1 ng λ-DNA as a template. Various sizes of alumina disks, ranging in diameter from 0 (no alumina membrane) to 6 mm, were immersed in the PCR tubes. **Fig. S1** (supplemental information) depicts the real time, fluorescent intensity as a function of time for these various cases.

The data was analyzed to determine the reaction efficiency $\boldsymbol{\varepsilon}$ as a function of the membrane's area. The number of PCR amplicons (N) after n cycles is $N = N_0 \cdot (1+\varepsilon)^n$, where N_0 is the amount of starting template, n is the number of PCR cycles, and ε is the efficiency ($0 \le \varepsilon \le 1$). The intensity of the fluorescence signal F is assumed to be proportional to N. Therefore, $\log F \propto n \cdot \log(1+\varepsilon)$, and the slope of the curve depicting $\log F$ as a function of n equals $\log(1+\varepsilon)$. Based on the real-time amplification curves of **Fig. S1**, **Fig. 3** depicts the normalized efficiency (%) as a function of the membrane's surface area during various cycling intervals. As the membrane's relative surface area increases, its inhibition effects increase and the PCR's efficiency decreases. In a separate set of experiments (not shown here), we demonstrated that the inhibitory effect can be partially offset for by increasing the amount of

enzyme, primers, and BSA in the PCR reaction mix. This is consistent with the hypothesis that PCR inhibition is due to membrane binding (and de-activation) of PCR reaction components.

3.2 Membrane Retention Efficiency

The DNA retention capacity of alumina membranes was previously studied [Kim *et al.*, 2006, 2008, and 2009] and it was demonstrated that 100 nm pores provide an optimal pore size for DNA binding. It is surmised that retention is a result of both physical filtration and chemical binding. As the solution salt concentration increased so did the membrane's DNA retention capacity. In the absence of salt, the 200 nm membrane retained 20% of genomic DNA. In the presence of 500 mM of salt, the retention was 75% [Kim *et al*. 2008].

Since typically the viral RNA molecule is significantly smaller than the bacterial genomic DNA fragments, we embarked on testing the membrane's retention capacity of the Armored HIV RNA molecules. In the absence of any salt in the buffer, the binding capacity for RNA was below 5%. The surface affinity of RNA increased significantly when high salt-based buffer was used. The Armored RNA retention fraction of the microfluidic-based membrane was 34±7% when the guanidine salt concentration was 4.5 M.

3.3 Bacterial DNA

The isolation and PCR amplification of bacterial DNA was tested using the Gram-positive bacteria *B. cereus* (genomic DNA 5,244,283 bp). For these tests, an AOM-PCR module with a reaction chamber volume of about 27 μl was used. The sample consisted of lysate (section 2.4) laden with bacteria concentrations ranging from 2.8×10^4 to 2.8×10^6 cells/ml. The amplicons (305 bp) were detected with EtBr-stained (2%) agarose gel electrophoresis. **Figure 4** is a gel image of the PCR products for a sample containing 3.1×10^4 cells (Lane 1), 3.1×10^3 cells (Lane 2), 3.1×10^2 cells (Lane 3) and a negative control, i.e., no *B. cereus* in the sample (Lane 4). Lane M is a marker VIII ladder. All the target-containing samples featured bands at the appropriate positions (consistent with 305 bp amplicons). Two tests were carried out at each target concentration with similar results.

3.4 Viral RNA

Isolation of RNA for RT-PCR was tested using Asuragen Armored RNA®, a safe surrogate for HIV. Lysis was performed outside the chip by incubation of an aliquot of Armored RNA with Qiagen AL buffer for 10 minutes. The primers targeted a 155 bp *gag* fragment of the HIV genome [Michael et. al, 1999]. The amplification products were detected with EtBr-stained agarose gel electrophoresis. **Figure 5** shows an agarose gel for RT-PCR amplicons, corresponding to sample template numbers of 2.0×10^4 (lane 1) and 2.0×10^3 (lane 2), respectively. Lane M is a marker VIII ladder. Negative controls (not shown) did not produce any band in the agarose gel. Both target-containing samples produced bands at the appropriate position for the amplicons (155 bp).

4. Conclusion

The design, fabrication, operation, and testing of a novel integrated, microfluidic module for combined nucleic acid isolation and amplification (PCR and RT-PCR) was demonstrated. The nucleic acid isolation and retention functions were carried out with an aluminum oxide, porous membrane that is embedded directly inside the PCR chamber. The integration of the membrane in the PCR chamber simplified the flow control and reduced the complexity of the diagnostic chip.

In contrast to prior work, we found that the alumina membrane plays some inhibitory role during the PCR amplification and care must be exercised to maintain the membrane's volume relative to the volume of the PCR chamber below a certain value.

Using EtBr-stained agarose gels to analyze PCR products, we detected nucleic acid targets isolated from lysates prepared from as few as 300 bacterial cells and 2000 synthetic virons. The relatively poorer performance with the RNA targets is attributed to the membrane's lower retention of RNA compared to that of DNA. Improved limits-of-detection could potentially be achieved with process optimization and the use of more sensitive PCR product detection methods.

The module described here can serve as a subsystem for a totally-integrated, sample-to-report microfluidic diagnostics system combining lysis, nucleic acid isolation, PCR or RT-PCR, and end-point detection of PCR products. For example, the PCR reagents can be wax-encapsulated and dry-stored in the PCR chamber [see Kim *et al*. 2009], and the PCR results can be detected in real time by adding appropriate dyes to the PCR mix.

ACKNOWLEDGMENTS

This work was supported, in part, by the NIH/NIDCR Grant U01DE017855.

References

B. Bowen and P. Durre [2003], *Nucleic Acid Isolation Methods* (American Scientific Publishers).

L. Burgoyne [2001], US Patent 6,294,203 “Dry medium for storage and analysis of genetic material” (September 25, 2001) and US Patent 6,322,983 “Solid medium and methods for processing genetic material (November 27, 2001).

M.C. Breadmore, K.A. Wolfe, I.G. Arcibal et al. [2003], "Microchip-based purification of DNA from biological samples" *Analytical Chemistry* **75** 1880-1886.

N.C. Cady, S. Stelick, and C.A. Batt [2003], "Nucleic acid purification using microfabricated silicon microstructures" *Biosensors & Bioelectronics* **19** 59-66.

X. Chen, K. Shen, P. Liu, M. Guo, J. Cheng, and Y. Zhou [2004], “Silica-based solid phase extraction of DNA on a microchip” *Tsinghua Science and Technology* **9, 4** 379-383.

Z. Chen, M.G. Mauk, J. Wang, W.R. Abrams, P.L. Corstjens, R.S. Niedbala, D. Malamud, and H.H. Bau [2007], “A microfluidic system for saliva-based detection of infectious diseases” *Annals of the New York Academy of Sciences* **1098** 429-436.

D. Chen, M. Mauk, X. Qiu, C. Liu, J. Kim, S. Ramprasad, S. Ongagna, W. R. Abrams, D. Malamud, P. L.A.M. Corstjens, and Haim H. Bau, 2010, "An Integrated, Self-Contained Microfluidic Cassette for Isolation, Amplification, and Detection of Nucleic Acids" accepted for publication in Biomedical Microdevices. DOI 10.1007/s10544-010-9423-4

L.A. Christel, K. Petersen, W. McMillan, and M.A. Northrup [1999], “Rapid, automated nucleic acid probe assays using silicon microstructures for nucleic acid concentration” *Trans. ASME* **121** 22-27.

S. Dames, L.K. Bromley, M. Hermann, M. Elgort, M. Erali, R. Smith, and K.V. Voelkerding [2006], "A single-tube nucleic acid extraction, amplification, and detection method using aluminum oxide" *J. Molecular Diagnostics* **8, 1** 16-21.

C.J. Easley, J.M. Karlinsey, J.M. Bienvenue, L.A. Legendre, M.G. Roper, S.H. Feldman, M.A. Hughes, E.L. Hewlett, T.J. Merkel, J.P. Ferrance, and J.P. Landers [2006], “A fully integrated microfluidic genetic analysis system with sample-in-answer-out capability,” *Proceedings Of The National Academy Of Sciences*, **103** 19272-19277.

M.G. Elgort, M.G. Herrmann, M. Erali, J.D. Durtschi, K.V. Voelkerding, and R.E. Smith [2004], “Extraction and amplification of genomic DNA from human blood on nanoporous aluminum oxide membranes” *Clinical Chemistry* **50, 10** 1817-1819.

M. Erali, J.D. Durtschi, K.V. Voelkerding, and R.E. Smith [2004], “Localization and imaging of nucleic acids on nanoporous aluminum oxide membranes” *Clinical Chemistry* **50, 10** 1819-1821.

E. W. Fiebig, D. J. Wright, B. D. Rawal, P. E. Garrett, R. T. Schumacher, L. Peddada, C. Heldebrant, R. Smith, A. Conrad, S. H. Kleinman, M. P. Busch, 2003, Dynamics of HIV viremia and antibody seroconversion in plasma donors: implications for diagnosis and staging of primary HIV infection, AIDS 17(13), 1871-9

J.C. Gerdes, J.M. Marmaro, and C.A. Roehl [2001], "Nucleic Acid Archiving" US Patent 6,291,166.

M.K. Hourfar, U. Michelsen, M. Schmidt, A. Berger, E. Seifried, and W.K. Roth [2005], "High-throughput purification of viral RNA based on novel aqueous chemistry for nucleic acid isolation" *Clinical Chemistry* **51:7** 1217-1222.

J. Kim, K. V. Voelkerding, and B. K. Gale [2006], "Patterning of a nanoporous membrane for multi-sample DNA extraction," *J. Micromech. Microeng.*, vol. 16, pp. 33-39.

J. Kim and B. K. Gale [2008], "Quantitative and qualitative analysis of a microfluidic DNA extraction system using a nanoporous AlOx membrane," *Lab on a chip*, vol. 8, pp. 1516 -1523.

J. Kim, M. Johnson, P. Hill, and B. K. Gale [2009], "Microfluidic sample preparation: cell lysis and nucleic acid purification," *Integr. Biol.*, vol. 1, pp. 574 -586.

J. Kim, D. Byun, M.G. Mauk, and H.H. Bau [2009], "A disposable, self-contained PCR chip" *Lab on a Chip* **9, 4** 606-612.

J. Kim, D. Chen, and H. H. Bau [2009], An automated, pre-programmed, multiplexed hydraulic microvalve, *Lab on a Chip*, **9,** 3594.

L.A. Legendre, J.M. Bienvenue, M.G. Roper, J.P. Ferrance, and J.P. Landers, "A Simple, Valveless Microfluidic Sample Preparation Device for Extraction and Amplification of DNA from Nanoliter-Volume Samples", *Anal. Chem.* 2006, 78, 1444-1451

P. Liu and R. Mathies [2009], "Integrated microfluidic systems for high-performance genetic analysis, *Trends in Biotechnology*, **27**, **10** 572-581.

X.J. Lou, N.J. Panaro, P. Wilding, P. Fortina, and L.J. Kricka [2004], "Increased amplification efficiency of microchip-based PCR by dynamic surface passivation" Biotechniques 36: 248-52.

R.L. Margraf, S. Page, M. Erali, and C.T. Wittwer [2004], "Single-tube method for nucleic acid extraction, amplification, purification, and sequencing" *Clinical Chemistry* **50:10** 1755-1761.

N. L. Michael, S. A. Herman, S. Kwok, K. Dreyer, J. Wang, C. Christopherson, J. P. Spadoro, K. K. Y. Young, V. Polonis, F. E. McCutchan, J. Carr, J. R. Mascola, L. L. Jagodzinski, and M. L. Robb, *J Clin Microbiol.*, vol. 37, pp. 2557-63, 1999.

B.L. Pasloske, C.R. Walkerpeach, R.D. Obermoeller, M. Winkler, and D.B. DuBois [1998], "Armored RNA technology for production of ribonuclease-resistant viral RNA controls and standards" *J. Clinical Microbiology* **36, 12** 3590-3594.

J. Wang, Z. Chen, P.L. Corstjens, M.G. Mauk, and H.H. Bau [2006], "A disposable microfluidic cassette for DNA amplification and detection" *Lab on Chip* **6, 1** 46-53.

K.A. Wolfe, M.C. Breadmore, J.P. Ferrance, M.E. Power, J.F. Conroy, P.M. Norris, and J.P. Landers [2002] "Toward a microchip-based solid-phase extraction method for isolation of nucleic acids" *Electrophoresis* **23** 727-733.

LIST OF CAPTIONS

1. AOM PCR chip. (A) Exploded view. All layers are polycarbonate plastic films (layers 1 and 3 are 0.25 mm thick; layer 2 is 0.8 mm thick; layer 4 is 0.5 mm thick). Conduits are located at the top side and the bottom side of layer 2. (B) Cross-sectional view showing the wax-sealed AOM in a cavity; (C) A photograph of the AOM PCR module.

2. A schematic depiction of the flow control of the AOM-PCR module: (A) nucleic acid binding; (B) washing and drying; (C) introduction of the PCR mix; and (D) thermal cycling.

3. Real-time PCR efficiency as a function of the area of membrane (mm^2) immersed in 25 μl PCR reaction volume. All reactions had the same amount of starting template, enzymes, and other components and were thermal cycled concurrently. The efficiencies were calculated at different stages of PCR process (cycles: 7-11; 10-15; 12-17; and 16-20).

4. An agarose gel (1.5 %) image of amplicons of *B. cereus* DNA. Lane M: a marker VIII ladder, lane 1: 3.1×10^4 cells, lane 2: 3.1×10^3 cells, lane 3: 3.1×10^2 cells and lane 4: a negative control.

5. An agarose gel (2 %) image of amplicons of armored RNA. Lane M is a marker VIII ladder. Lane 1: 2.0×10^4 copies and lane 2: 2.0×10^3 copies

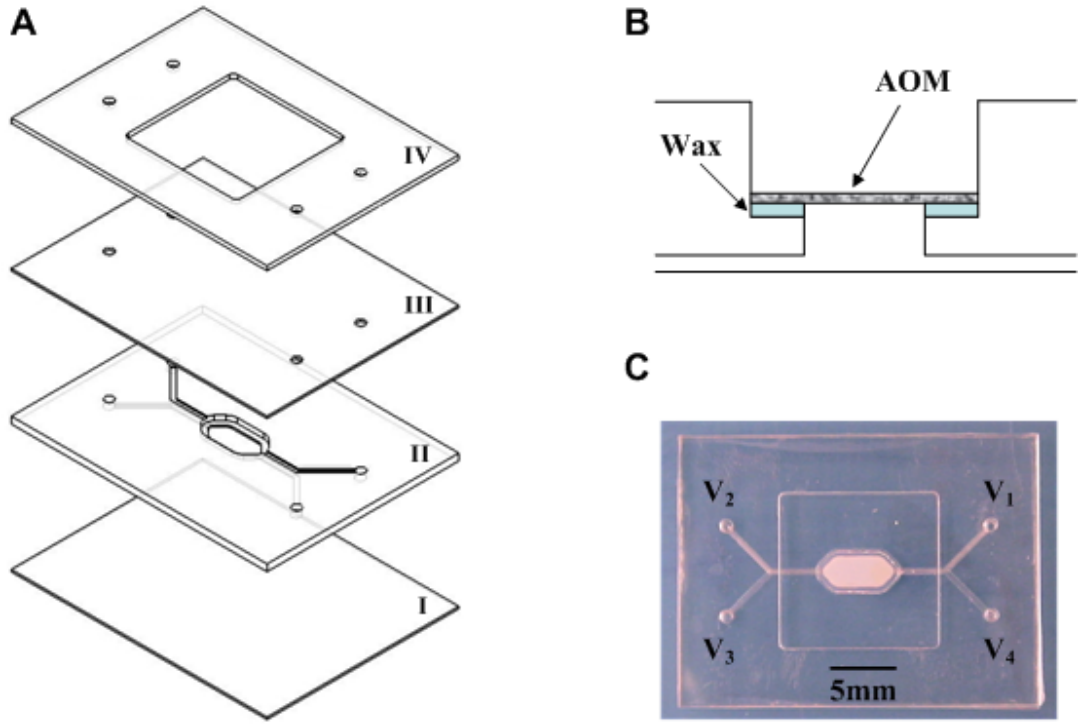

Fig. 1: AOM PCR chip. (A) Exploded view. All layers are polycarbonate plastic films (layers 1 and 3 are 0.25 mm thick; layer 2 is 0.8 mm thick; layer 4 is 0.5 mm thick). Conduits are located at the top side and the bottom side of layer 2. (B) Cross-sectional view showing the wax-sealed AOM in a cavity; (C) A photograph of the AOM PCR module.

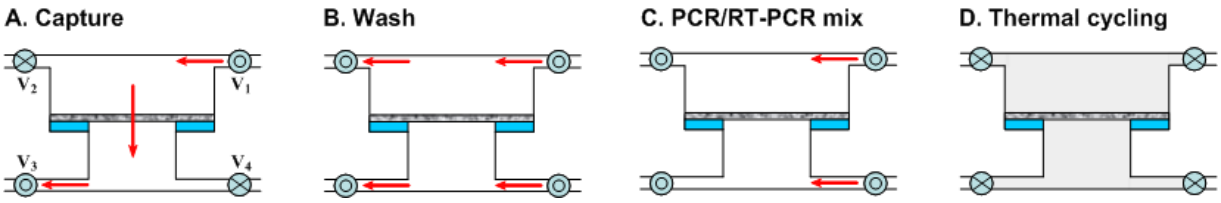

Figure 2: A schematic depiction of the flow control of the AOM-PCR module: (A) nucleic acid binding; (B) washing and drying; (C) introduction of the PCR mix; and (D) thermal cycling.

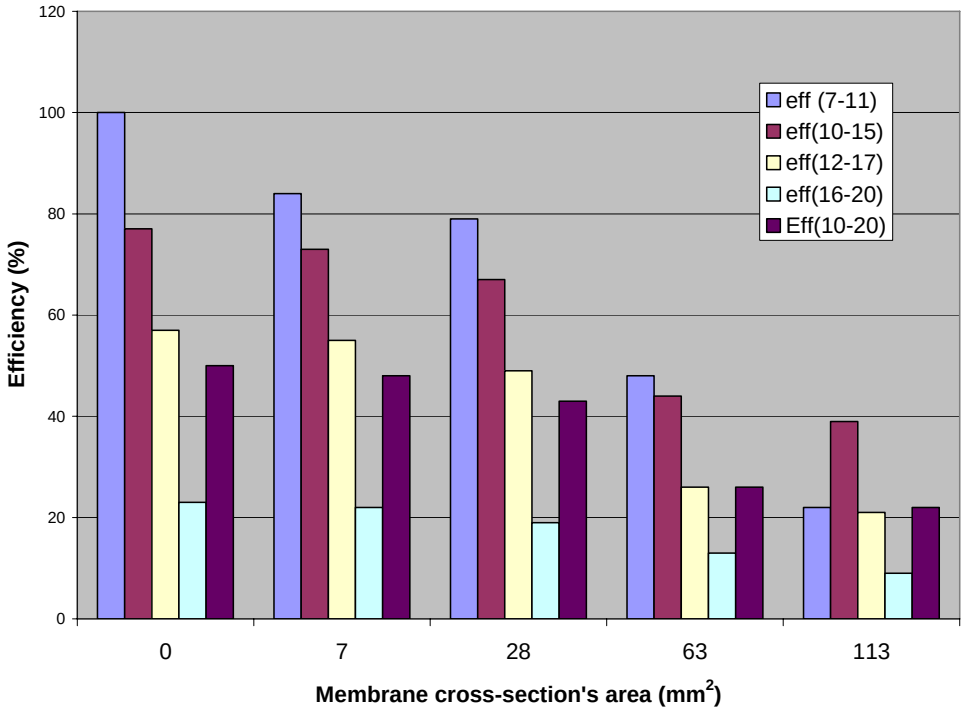

Fig. 3: Real-time PCR efficiency as a function of the area of membrane (mm^2) immersed in 25 µl PCR reaction volume. All reactions had the same amount of starting template, enzymes, and other components and were thermal cycled concurrently. The efficiencies were calculated at different stages of PCR process (cycles: 7-11; 10-15; 12-17; and 16-20).

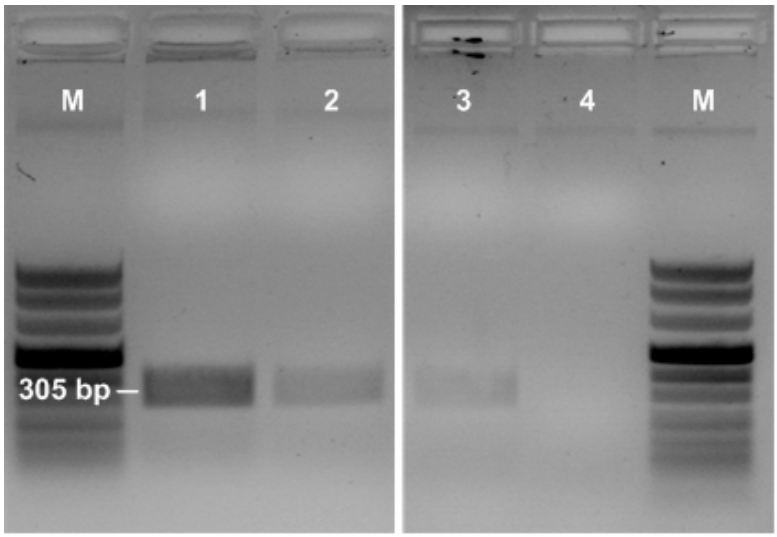

Fig. 4: An agarose gel (1.5 %) image of amplicons of *B. cereus* DNA. Lane M: a marker VIII ladder, lane 1: 3.1×10^4 cells, lane 2: 3.1×10^3 cells, lane 3: 3.1×10^2 cells and lane 4: a negative control.

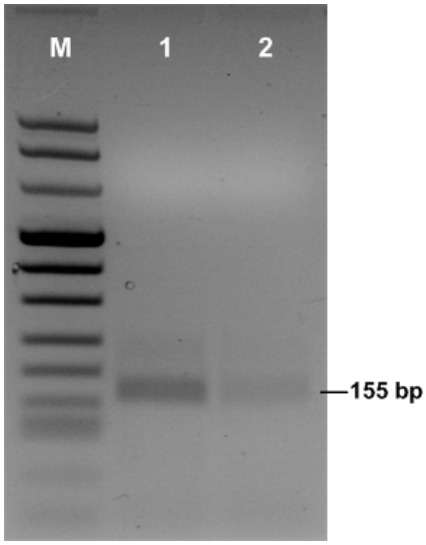

Fig. 5: An agarose gel (2 %) image of amplicons of armored RNA. Lane M is a marker VIII ladder. Lane 1: 2.0×10^4 copies and lane 2: 2.0×10^3 copies